Journal of Structural Geology 32 (2010) 656–666

Contents lists available at ScienceDirect

Journal of Structural Geology

journal homepage: www.elsevier.com/locate/jsg

Structure and development of an anastomosing network of ductile shear zones

Jordi Carreras [a,*], Dyanna M. Czeck [b], Elena Druguet [a], Peter J. Hudleston [c]

[a] Departament de Geologia, Universitat Autònoma de Barcelona, 08193 Bellaterra, Barcelona, Spain
[b] Department of Geosciences, University of Wisconsin-Milwaukee, P.O. Box 413, Milwaukee, WI 53201, USA
[c] Department of Geology and Geophysics, University of Minnesota, Minneapolis, MN 55455, USA

ARTICLE INFO

Article history:
Received 23 July 2009
Received in revised form
3 March 2010
Accepted 30 March 2010
Available online 7 April 2010

Keywords:
Anastomosing shear zones
Conjugate shears
Geometry
Kinematics
Metagabbro
Mylonite

ABSTRACT

A detailed structural analysis of an anastomosing shear zone network in metagabbros from the Archean Rainy Lake zone (Canada) revealed the existence of prevalent dextral and minor sinistral conjugate shear zones with the obtuse angle (>130°) facing the main shortening direction. A typology of shear zone intersections, confluences, and other features shows that all shears formed during a single deformation event, with dextral and sinistral shears being active together or in an alternating fashion. In spite of the difficulty of establishing a complete kinematic sequence, early and late shears can be distinguished. The final angular pattern between dextral and sinistral shears is not an original feature. Dextral and sinistral shears formed at nearly right angles, and the angles progressively opened towards the extension direction as a result of increasing strain. The obtuse angles were achieved by the combined effects of continued shearing on newly forming shears and internal deformation of the lozenge-shaped domains of lesser-deformed rock bounded by the shears. Through time, there was an increasing prevalence of dextral shears over sinistral ones. The studied pattern and sequential analysis indicate that the bulk deformation was noncoaxial with a deformation regime evolving from a pure shear-dominated dextral transpression to a higher vorticity dextral transpression.

1. Introduction

Ductile shear zones and brittle shear fractures accommodate deformation in a wide variety of rock types. Shear fractures often consist of many linked smaller fractures (Wilcox et al., 1973; Cundall, 1991; Olsson et al., 2004; Kim et al., 2004). Although individual shear zones are usually defined as planar bands of deformation surrounded by less deformed or undeformed rocks (e.g., van der Pluijm and Marshak, 2003), they may often be nonplanar and link together in a pattern of anastomosed networks with rather complicated geometries that bound undeformed or less deformed lozenges (Ramsay and Graham, 1970; Mitra, 1979, 1998; Ramsay and Allison, 1979; Bell, 1981; Choukroune and Gapais, 1983; Gapais et al., 1987; Burg et al., 1996; Corsini et al., 1996; Hudleston, 1999; Arbaret et al., 2000; Carreras, 2001; Czeck and Hudleston, 2003, 2004; Bhattacharyya and Czeck, 2008). These geometrical organizations of shear zones are of primary importance as they have been called upon to partially control both strain accumulation (e.g., Hudleston, 1999) and deformation mechanisms (e.g., Fusseis et al., 2006).

Whereas the formation and development of networks of brittle shear fractures are well documented in the literature (e.g., Wilcox et al., 1973; Maerten et al., 2002), less information on the progressive development of ductile or brittle–ductile shear zones and the interaction between shear zone strands exists (Carreras et al., 2000; Pennacchioni and Mancktelow, 2007).

When evaluating a network of shear zones, field geologists often look at the second order features to determine the temporal relationships between the strands. For example, shear zone thickness may be considered roughly proportional to age (Mitra, 1979), although caution is necessary when using this approach because the rheology of the material (i.e., strain hardening vs. strain softening) will affect this relationship (Hull, 1988; Means, 1995; Schrank et al., 2008).

The pattern of interrelated natural ductile shear zones varies considerably, from fairly regular conjugate pairs (Lamouroux et al., 1991) to sets that may have an octahedral arrangement (Mitra, 1979), to more complicated and less regular patterns of interconnectedness (Bhattacharyya and Hudleston, 2001). Some studies have indicated a similarity between the temporal evolution of ductile shear zone strands and brittle shear zones (Lamouroux et al., 1991). However, the two types of structures may evolve differently due to the differences in the active deformation mechanisms and the strain compatibility requirements in ductile shear zones. Schwarz

* Corresponding author. Fax: +34935811263.
E-mail address: jordi.carreras@uab.cat (J. Carreras).

0191-8141/$ – see front matter © 2010 Elsevier Ltd. All rights reserved.
doi:10.1016/j.jsg.2010.03.013

and Kilfitt (2008) conducted analogue experiments of conjugate fault systems and demonstrated that the kinematics become more complicated as deformation progresses. In particular, directions of fault propagation are influenced by motion along neighbouring faults, and dominant activity alternates between neighbouring faults. A similar progression of alternating active strands may occur in the ductile shear zones. In order to understand the evolution of shear zone sets with a numerical approach, Mancktelow (2002) tested the effect of different rheologic parameters and deformation geometries in the development of conjugate shear zone systems and found that typically, conjugate shear zones initiate at approximately perpendicular orientations, and rotate with increasing bulk deformation. These experimental results also elucidate some of the difficulties in understanding shear zone network evolution. In particular, the relative timing of different shear zones may be difficult to establish because, in some instances, much like in brittle fault networks, the displacement along different shears has a pulsating character, shifting from one to another.

Overall strain accumulation will be controlled both by the shear zones themselves, the interactions between shear zones, and the amount and type of strain that is partitioned into the wall rocks and at the interior of shear-bounded lozenges. One of the main differences between brittle and ductile shear networks is that in the latter, the angle facing the mean shortening direction may increase with progressive deformation (Mitra, 1979; Ramsay and Huber, 1987). This angular evolution cannot be achieved merely by passive rotation of the shear zones because strain compatibility requires contemporaneous internal deformation of the shear-bounded domains. In most cases, strain compatibility is maintained by a combination of strain within the shear zones, strain localization producing new shear zones, and internal deformation of the lozenges. Simultaneous rotation of initial shears plus the propagation of new ones merging with pre-existing ones results in the typical network consisting of anastomosing shear zones and lozenges.

Several authors have considered geometrical configurations and strain accumulation in and near shear zone networks. Gapais et al. (1987) described shear zone patterns that they interpreted to reflect the symmetry of the bulk strain, orthorhombic in the case of coaxial deformation and lower symmetry for noncoaxial deformation. They suggested that the individual shear zones tend to track surfaces of no finite deformation. In contrast, Mitra (1979) treated individual shears as markers that initiated at 90° on principal planes and rotated during deformation of the surrounding rock mass. Hudleston (1999) examined three-dimensional arrays of shear zones and determined that the evolving network geometries are inextricably linked to the maintenance of strain compatibility.

The intersection points of shear zones within networks are loci for complex strain accommodation and potential secondary structures. Lamouroux et al. (1991) developed a theoretical analysis of geometrical compatibility constraints at domains of intersecting conjugate natural shear zones. Based on their analysis, shear zone networks should evolve in the same sequence as brittle shear networks, but the strains at the intersection regions are more complex. Pennacchioni and Mancktelow (2007) further demonstrated with a field example the complex strains and the compatibility problems at conjugate shear zone intersection points. Harris (2003) documented further complexities that can occur when shear zones interact, explaining the geometry and the kinematics of back-rotated folds that occur within shear-bounded lozenges when the bounding shear zones come into close proximity. In fact, other studies have similarly concluded that many lozenges in ductile networks contain some type of internal deformation (Bell, 1981; Treagus and Lan, 2000; Pennacchioni and Mancktelow, 2007; Jessell et al., 2009).

Despite these advances, key questions concerning the structure and evolution of anastomosing patterns of shear zones remain including: (i) What are the initial orientation and kinematics of the sets? (ii) How are strain and kinematic compatibility maintained at the domains of merging shear strands? (iii) How do the sets evolve geometrically and kinematically during progressive deformation? (iv) In what orientations are new shears or sets added? (v) What is the behaviour (internal deformation and/or rigid body rotation) of shear-bounded lozenges? All of these questions could be addressed from the analysis of naturally deformed examples from the micro- to the macro-scale.

This paper describes a process-oriented study based on a detailed analysis of a single outcrop containing an anastomosed shear zone network developed in metagabbroic rocks. The main purpose is to establish criteria for the relative timing of individual shears based on our own field observations complemented with the criteria deduced by Schwarz and Kilfitt (2008) for conjugate faults. We also demonstrate the use of the shear zone criteria in a field example.

One difference between our case study and most experimental models is that in the studied field example, shearing generates foliated rocks (mylonite bands) that might themselves be affected by progressive deformation. In experimental models, shears are generally more discrete and do not generate wide domains with a new mechanical anisotropy. One might consider the formation of foliation to be one more complicating factor. However, the shear-induced foliation also simplifies the analysis because it acts as a new marker in the rock. Thus, in such situations a shear strand deforming a mylonitic foliation clearly post-dates the shear event that caused the initial mylonitic foliation.

2. Geologic setting

2.1. Regional geology

The studied shear zone network is located in the Rainy Lake region within the Superior Province on the border of Ontario, Canada and Minnesota, USA. The Superior Province is a part of North America's Precambrian craton and can be divided into several subprovinces based on lithological and structural contrasts (Card and Ciesielski, 1986), with more recent work including the concept of tectonic terranes (Percival et al., 2006). The Rainy Lake region is a fault/shear zone bounded triangular wedge that straddles one such boundary between the Wabigoon granite–greenstone subprovince and the Quetico metasedimentary subprovince (Card and Ciesielski, 1986; Poulsen, 1986; Fig. 1a). The tectono-metamorphic features of this boundary zone are the response to the late Archean oblique terrane collision (Kenoran orogeny) which occurred at about 2.69–2.7 Ga (Stockwell, 1982; Davis et al., 1989; Fralick et al., 2006). The region has been largely unaffected by subsequent tectonic events.

The faults that bound the Rainy Lake wedge separate the mostly amphibolite grade metasedimentary rocks in the Quetico subprovince from the mostly greenschist grade metavolcanic and plutonic rocks in the Wabigoon subprovince (Poulsen, 2000). The primary fault/shear zone is the Quetico Fault, which extends for several hundred km along the subprovince boundary. The triangular wedge is created by the intersection of the Quetico Fault with the Rainy Lake–Seine River Fault (Poulsen, 1986). The Rainy Lake zone contains allochthonous blocks of varying lithologies that were brought together along structurally discordant boundaries and rocks that were formed in response to the dynamic tectonic environment of oblique terrane collision (Poulsen et al., 1980; Davis et al., 1989; Poulsen, 2000; Druguet et al., 2008; Fig. 1).

The area between the two major shear zones contains a complex pattern of anastomosing subvertical shear zones and fabrics wrapping around gneiss domes and granitoid plutons (Poulsen, 2000; Czeck and Hudleston, 2003, 2004; Druguet et al., 2008). The studied

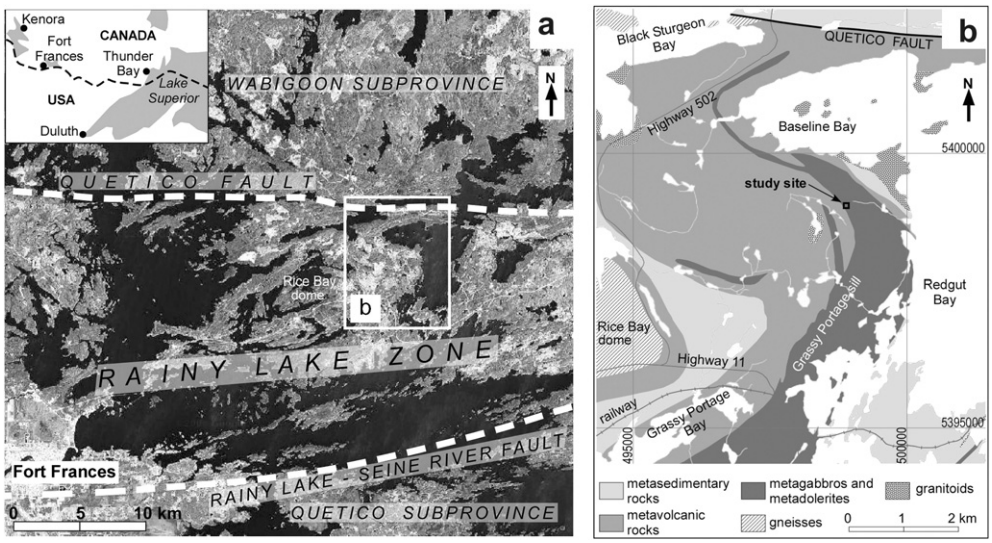

Fig. 1. Setting of the study area. (a) Satellite photograph of the boundary between Wabigoon and Quetico subprovinces in the Rainy Lake zone, with the main boundary fault-zones depicted in dashed lines. Source: GoogleEarth. (b) Geological map of the area around the Grassy Portage sill, based on map by Poulsen (2000). The grid refers to the Universal Transverse Mercator coordinate system (U.T.M., WGS84 datum).

shear zones lie directly to the northeast of one such gneiss dome, the Rice Bay Dome (Poulsen, 2000; Druguet et al., 2008). The structural patterns can be explained by an overall dextral transpressive tectonic regime with sub-horizontal NW–SE shortening (Poulsen, 1986, 2000; Tabor and Hudleston, 1991; Borradaile and Dehls, 1993; Borradaile et al., 1993; Czeck and Hudleston, 2003; Druguet et al., 2008).

Peak metamorphic conditions included temperatures that ranged from 400 °C to 600 °C, with pressures of approximately 300 MPa (Poulsen, 2000). Within the Rainy Lake region, the rocks are generally greenschist facies to the east and mid-amphibolite facies to the west (Poulsen, 2000). Within our small field example, the rocks are within the amphibolite facies domain. The continuation of the dextral transpressive event towards retrograde metamorphic conditions led to strain localization along the two major dextral shear zones, but also along narrow mesoscale shears (Poulsen et al., 1980; Poulsen, 2000). Discrete shear zones were particularly developed in plutonic rocks including metatonalites and metagabbros, giving rise to mylonites.

The allochthonous nature of most rocks within the wedge and the dynamic nature of the tectonic environment where syntectonic rocks were formed resulted in a wide variety of distinct lithological units including interlayered sequences of ultramafic to felsic metavolcanic rocks, metasedimentary rocks (mostly metagreywackes and metapelites), metagabbroic and metadoleritic intrusions, felsic orthogneisses, and syntectonic granitoids with associated networks of leucocratic veins (Poulsen et al., 1980; Davis et al., 1989; Poulsen, 2000; Czeck et al., 2006; Druguet et al., 2008).

The studied shear zones are contained within one of the most prominent mafic intrusions in the area, a large metamorphosed layered gabbroic sill, the Grassy Portage intrusion, which is exposed approximately 20 km along its strike and has been overturned so that it dips steeply to the northwest (Poulsen, 2000). The foliation within this sill and other neighbouring rocks is deflected from the typical NE–SW regional strike to a N–S and WNW–ESE orientation due to proximity to the Rice Bay Dome.

2.2. Gabbro host rock

Within the Grassy Portage sill, layering is defined by variations in mineralogy and chemistry, both regionally (km scale) and locally (cm scale) (Poulsen, 2000). Compositions range from melagabbro to anorthosite (Poulsen, 2000). The margins of the Grassy Portage sill have been exploited for disseminated chalcopyrite and pyrrhotite mineralization (Poulsen, 2000).

The specific studied outcrop is located along the base (northwest margin) of the sill (Fig. 1b). This lower portion of the sill is dominated by the compositions of gabbroic and anorthositic rocks that either may have formed by gravitational setting or autointrusion (Poulsen, 2000). The metagabbroic rocks range from leucogabbro to gabbro in composition and are dominantly poikilitic cumulates with hornblende megacrysts surrounding finer grains of plagioclase with minor amounts of chlorite and biotite (Poulsen, 2000). Equigranular gabbros containing hornblende, plagioclase, and minor amounts of chlorite and biotite are also present. The anorthositic rocks are often lenticular enclaves or pods within the gabbros (Poulsen, 2000). In neighbouring regions, the anorthositic pods have adcumulate textures of fine-grained andesine grains (Poulsen, 2000). At this outcrop, the pods are primarily adcumulates composed of fine-grained zoisite, presumably hydrously altered plagioclase as evidenced by some relict plagioclase grains, with quartz and minor amounts of calcite. The pods have generally ellipsoidal or lenticular shapes and range in size up to 50 cm maximum diameter. Both the gabbros and the anorthosites are affected by subsequent small-scale (cm–dm) shear zones, creating a foliated mylonitic fabric. These shear zones are the focus of our study.

3. Structure

3.1. The anastomosed shear zone pattern

The studied outcrop is a sub-horizontal glaciated surface, exposing an anastomosing network of predominantly NNW–SSE striking, moderately to steeply dipping shear zones (Fig. 2). The metagabbros exhibit an undulate pre-shearing weak foliation striking approximately 110° and steeply dipping, formed by aligned amphiboles and linked amphibole crystals. The orientation of this local foliation is consistent with the prevailing foliation in the immediate region, which is steep and appears to "wrap" around the Rice Bay Dome (Fig. 1).

The shear zones are defined by deflection and intensification of this prevailing foliation. They are narrow and discrete bands, with

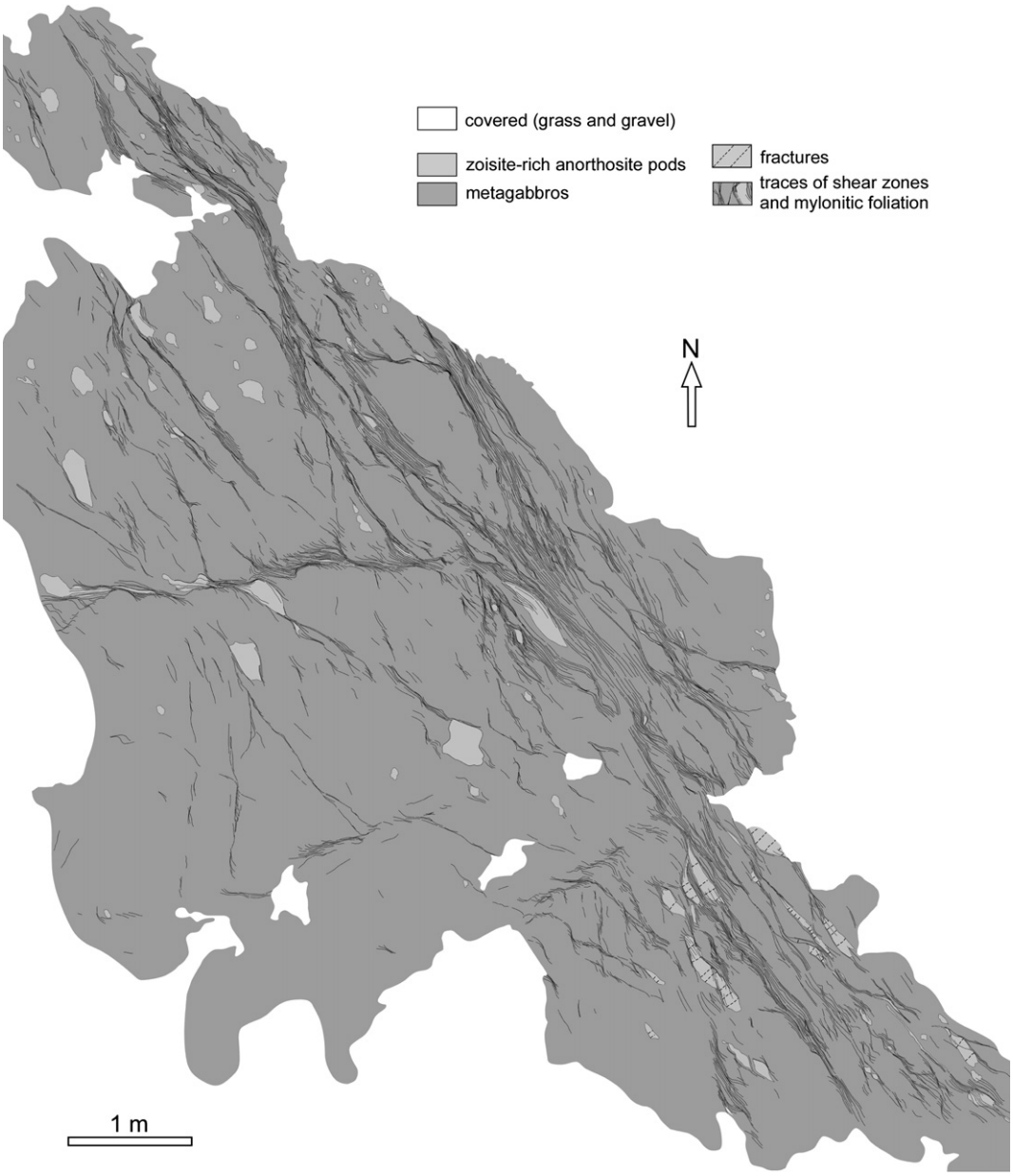

Fig. 2. Detailed map of the studied outcrop. Location in the Universal Transverse Mercator coordinate system (U.T.M., WGS84 datum) is $X = 498889$, $Y = 5399130$.

a maximum width of a few centimetres, that define an anastomosed pattern. Inside the shear zones, the rocks are well-foliated and fine-grained mylonites (Fig. 3). The shear zones are preferentially within the gabbros and often localize at the gabbro/pod margins (Fig. 3b). However, the shear zones also cut across some pods where they are defined by mylonitic banding with finer grain size and segregated compositional banding. Foliation deflections at the shear zone margins enabled us to establish the sense of shear movement in most cases.

In spite of the predominance of two-dimensional outcrop surfaces, some morphological steps parallel to the shear zones enable views of sub-horizontal stretching lineations formed by aligned amphiboles. We interpret the lineations to be consistent with sub-horizontal strike-slip motion along the shear zones. Thus, the sub-horizontal outcrop surface is roughly parallel to the shear direction and appropriate for our kinematic analysis. The azimuth of the overall average strike of the anastomosed shear zone network is 150°, although the network is composed of shear zones ranging in strike from 60° to 180°. Based on the foliation deflection patterns, two main sets of shear zones, dextral and sinistral, can be distinguished. The dextral set outnumbers the sinistral set. Both sets exhibit a range of orientations. Three-dimensional analysis on a stereonet (Fig. 4) shows that the average trends of the dextral and sinistral sets form an obtuse angle of $\approx 135°$, with the shortening direction facing that obtuse angle between the two sets. Stretching lineations form two maxima at high angles to the intersection line between the two sets of shear zones (Fig. 4). Although this geometry is predicted for conjugate systems, it differs from similar settings (Ramsay and Allison, 1979, their Fig. 10; Carreras and Losantos, 1982; Carreras et al., 2004, their Fig. 2b) where the lineations form a unique maximum closely parallel to the intersection line of the shear zone planes.

Fractures are the latest structures, cutting both the foliation and shear zones (Fig. 3b). They are located exclusively in the

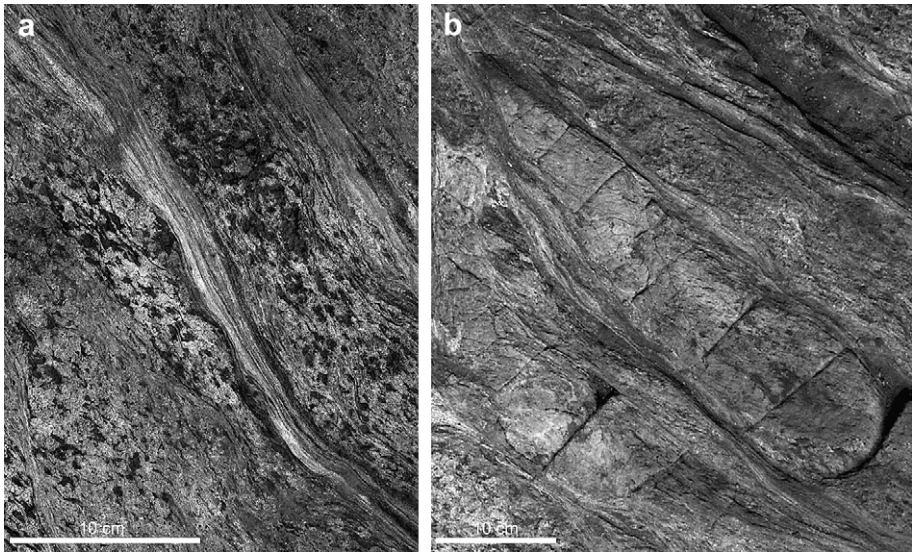

Fig. 3. (a) Two fine-grained mylonitic bands associated with dextral shears that cut across gabbros with variable degrees of mylonitization. The gabbros exhibit a slightly oblique, less penetrative mylonitic foliation. (b) Late extensional fractures affecting a mylonitic zoisite-rich anorthosite pod. North is upwards in both (a) and (b).

transformed anorthosite (zoisite) pods and are chiefly oriented transverse to the mylonitic foliation. The regularity of the fracture orientations suggests that they formed in response to the final state of instantaneous strain because one would only expect them to be subparallel if they formed without any subsequent rotation. They are interpreted as extensional (Mode I) fractures.

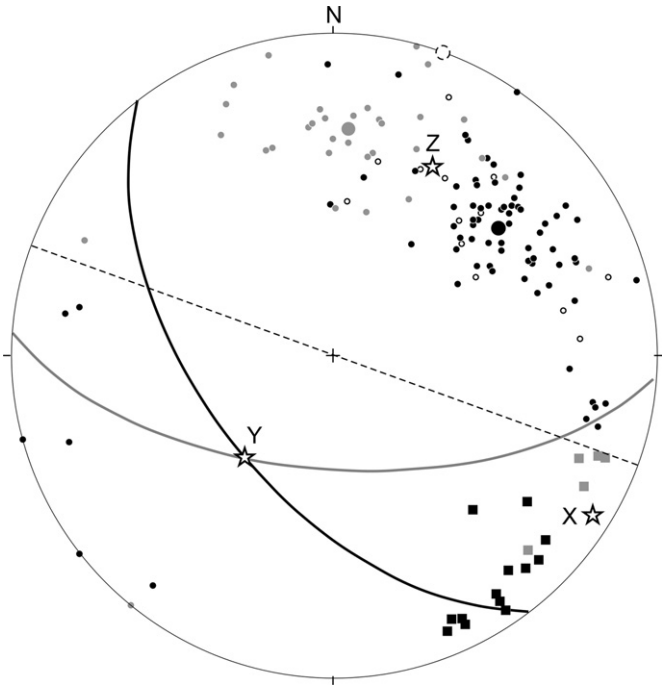

Fig. 4. Equal area stereoplot showing the orientation of shear zones. Circular dots are poles to mylonitic foliation or discrete shear zone planes (black for dextral, grey for sinistral and blank for uncertain shear sense). The great circles and large dots indicate the corresponding mean planes and their associated poles. Dashed line and circle correspond respectively to the main plane and pole to pre-shearing weak foliation in the metagabbros. Squares correspond to the respective stretching lineations. Stars indicate the inferred maximum bulk finite stretching axes (*X*, *Y* and *Z*). The obtuse angle between the mean shear planes is $\approx 135^{\circ}$.

3.2. Intersections and confluences: typology

It is a priori almost impossible to deduce the whole sequence of shear pulses in an anastomosed network of penecontemporaneous shear zones. However, experimental data show that not all individual shears are simultaneously active (Williams and Price, 1990; Carreras et al., 2000; Mancktelow, 2002). In this respect, ductile shear zone arrays are similar to brittle fault networks (e.g., Schwarz and Kilfitt, 2008). Individual analyses of shear zone confluences or intersections allow establishment of a relative time sequence based on geometric criteria. This is more manageable when, as in the present situation, one deals with ductile shear zones developing a mylonitic foliation. In this case, it can be assumed that instabilities that affect the mylonitic planar fabric post-date it. However, some caution is needed because in many instances, the initially developed fabric may have had a nonplanar geometry. For example, this is the case when the former foliation wraps around a relatively more competent pod. However, with careful analysis, it is possible to separate original foliation perturbations from perturbations arising from non-coeval shearing at confluence or intersection domains. Therefore, prior to our analysis, we present a typology of observed geometries enabling the establishment of relative timing of shears.

3.2.1. Cross cuts

This is an unquestionable setting where a shear zone is deformed and displaced by another. In our field example, dextral shear zones cut sinistral ones (Fig. 5) and vice versa.

3.2.2. Wedged coalescences

This is a common situation observed in other shear zones and on all scales (Duebendorfer and Christensen, 1998; Passchier and Coelho, 2006; Druguet et al., 2009). The wedge-inducing shears (secondary shears) can be antithetic (Fig. 6a,b) or synthetic (Fig. 6c) with regard to the older and wider mylonitic zone. The secondary shears form preferentially or exclusively at sharp boundaries and dissipate into the lozenge interior. Our interpretation is that these shears nucleate at the mylonitic/non-mylonitic interface and propagate towards the lozenge interior while the surrounding mylonitic fabric deflects to form a wedge shape.

Fig. 5. Line drawing of an early sinistral shear zone cut by sets of late dextral shears. Although it cannot be excluded that some pulses of sinistral shearing succeeded or accompanied dextral shearing, most of the sinistral shearing preceded the dextral shearing.

3.2.3. Internal shears

Mylonitic foliation is often internally affected by second order shears including shear bands (White et al., 1980; Carreras, 2001; Passchier and Trouw, 2005; Fusseis et al., 2006). The second order shears are generally synthetic and overprint the pre-existing mylonitic foliation (Fig. 7), so it is obvious that they post-date the pre-existing foliation.

3.2.4. Confluences

This is the most complicated situation, in which it may be difficult to determine the relative timing. In many examples (Fig. 8a), the wider shear zone exhibits more complex internal structures, possibly indicating a longer kinematic history. These complexities support the assumption that wider and longer shears predate the shorter and narrower ones in situations where the rocks are rheologically homogeneous. In other examples, like the one shown in Fig. 8b, two long and wide shear zones join, and it is not possible to deduce the relative timing.

3.2.5. Other structures

Older shears are generally broader and display abundant perturbations, and these criteria also may allow discrimination of relative timing. In addition to overlapping (superimposed shears), the presence of folds affecting the mylonitic foliation (Bell, 1978; Ghosh and Sengupta, 1987; Alsop and Holdsworth, 2002; Carreras et al., 2005) is a distinctive feature found in shear zones with a long and complex shear history (Fig. 9a). The shearing may be assigned to a relatively early stage if the entire shear zone itself is folded. To accommodate such folding, the lozenge itself must undergo internal ductile deformation along its margin (Fig. 9b). Small shears may instead form entirely isolated within the undeformed lozenges (Fig. 10). They likely arise due to the accommodation of deformation induced by the larger shears outside the lozenges in order to maintain strain compatibility. Therefore, they are expected to have formed late in the deformation, but this timing relationship is inconclusive. It is also possible that they formed early and became inactive as neighbouring shears more favourably aligned or more effectively accomplished the deformation by strain softening, thus causing them to become frozen in an incipient state of development, similar to the way in which larger brittle fractures inhibit the propagation of adjacent smaller fractures (Pollard and Aydin, 1988).

4. Kinematic analysis and interpretation

Several problems arise in the interpretation of the development of sets of conjugate systems of brittle–ductile and ductile shear zones. First, the angle facing the maximum bulk shortening direction may vary from acute (Lamouroux et al., 1991) to nearly straight

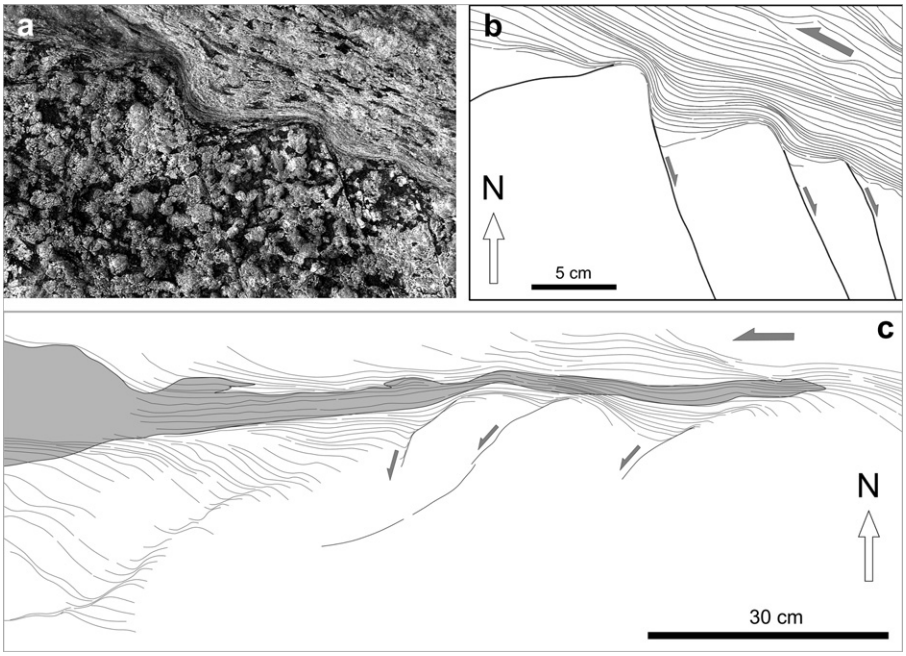

Fig. 6. Line drawings of wedged coalescences. Photograph (a) and interpretative sketch (b) of an early broad sinistral mylonitic band wedged as a consequence of a merging set of late antithetic discrete dextral shears. (c) Synthetic shears merge into a previously existing broader sinistral shear. Anorthosite is depicted in grey.

Fig. 7. Examples of internal shears (line drawings). (a) Synthetic sinistral shear bands. (b) Synthetic dextral shears bands. An anorthosite pod is depicted in grey.

(Carreras, 2001, his Fig. 16; Montomoli et al., 2008), although obtuse angles prevail (Ramsay, 1980; Gapais et al., 1987; Marquer et al., 1996). Second, compatibility problems arise from the impossibility of simultaneous shearing of two intersecting shear zones (Ramsay and Huber, 1987). A third complication arises from the fact that often the bulk deformation is not uniquely accommodated by shears, but also by the internal deformation of the shear zone bounded lozenges. The internal deformation of the lozenges is not necessarily homogeneous but can also be accommodated by internal shears like the one shown in Fig. 10.

4.1. Bulk geometry and kinematics

The following analysis will be performed on the basis of shear zone orientation and kinematics because of the difficulty of determining the deformation and rotation of the lozenges.

As shown in Figs. 4 and 11a, both dextral and sinistral shears are present, but dextral shears predominate. The average angle between both sets is ≈135°. Each set includes shears that recorded activity in earlier and late stages of the deformation, although the relative importance of dextral over sinistral increases in later stages. The average angle between early sets is ≈140° (132° on the outcrop surface, Fig. 11a), whereas for the late sets this is smaller (≈90°, 74° on the outcrop surface). For both sets, the later shears are oriented differently than the earlier shears. For the dextral set, later shears are clockwise oriented with regard to older ones, while the opposite occurs for the sinistral set (Fig. 11a).

4.2. Sequential development

For each set of shears, the final orientations are likely the product of rotation, particularly for the older dextral and sinistral sets (Fig. 11b). We assume that the later sets have not rotated significantly since their formation. Therefore, we further assume that the initial angle between sets that faced the bulk shortening direction was ~90°, similarly to conjugate sets that form at nearly perpendicular orientations, as described in other studies (Ramsay and Huber, 1987; Mancktelow, 2002). As deformation progressed, the two sets rotated in opposite directions. The dextral set rotated in a counterclockwise direction and, by a relatively larger amount, the sinistral set rotated in a clockwise direction, so that the angle between them increased over time (Fig. 11b). The rotations of older shears and the continuing development of new shears caused the complex intersecting geometries that we observe today.

The above inferred angular changes allow us to estimate the amount of strain recorded after the onset of the early shear sets. Assuming coaxial deformation, such a change in angle corresponds

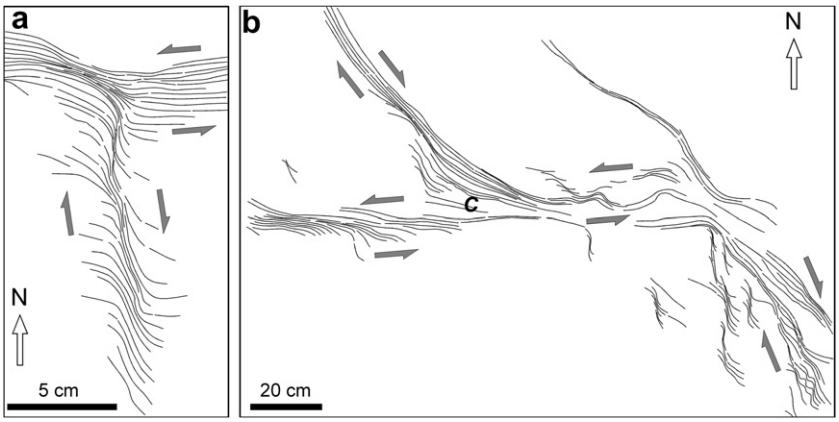

Fig. 8. Examples of shear zone confluences (line drawings). In (a) A minor N–S dextral shear zone merges into a wide sinistral E–W trending one. The E–W shear zone likely had a longer kinematic history. (b) Two merging dextral and sinistral wide early shear zones (confluence domain is labelled with a "C"). Both examples illustrate the common difficulty of establishing relative timing.

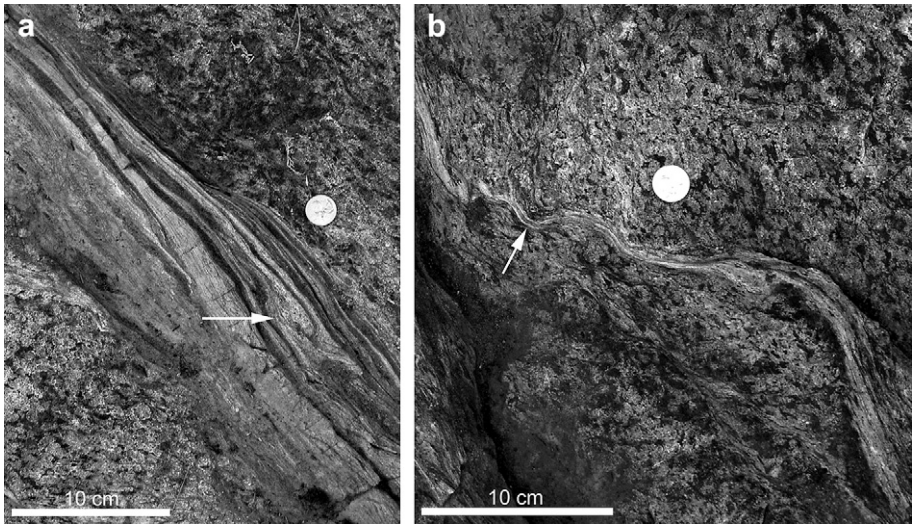

Fig. 9. Folds within shear zones. North is upwards. (a) Folds (arrow) affect the shear zone related mylonitic foliation. (b) The shear zone and mylonitic foliation are both folded (arrow) by the effect of later shear zone development. Both examples are distinctive characteristics of shears developed at early stages of the deformation and subjected to later perturbations.

to a 40% sub-horizontal NE to NNE shortening. This amount would be somewhat higher ($\approx$50%) for a slightly noncoaxial deformation. This shortening value has been inferred for the studied area that represents a relatively high strain domain bounded by less deformed metagabbros. Thus, the obtained shortening magnitude is not representative of bulk shear-related deformation affecting the entire Grassy Portage sill.

The fact that both dextral and sinistral sets rotated in opposite senses suggests an important component of shortening in bulk deformation. A bulk coaxial shortening would not explain the large prevalence of the dextral set, unless the effects of the previous anisotropy is considered (Cobbold et al., 1971; Gómez-Rivas et al., 2006). In this case, the obliquity between the pre-existing foliation plane and the bulk *XY* plane ($\approx$34°, Figs. 4 and 11b) could account for the prevalence of the dextral set. However, continuing coaxial deformation would cause the final development of a pattern of equally dominant dextral and sinistral sets, which is not the case. At the late stage, 85% of shears are dextral and most of them are of the shear band-type, which together indicate the presence of a bulk dextral shear component. Conversely, the early sinistral set is segmented by later cross-cutting shears, and it contains a greater dispersion of orientations, indicating that the sinistral orientations were unstable and that their activity decreased in time. The increased dominance of dextral shears in the later group is consistent with an evolution to transpression with higher vorticity, which is compatible with the sub-horizontal stretching lineation found at this outcrop.

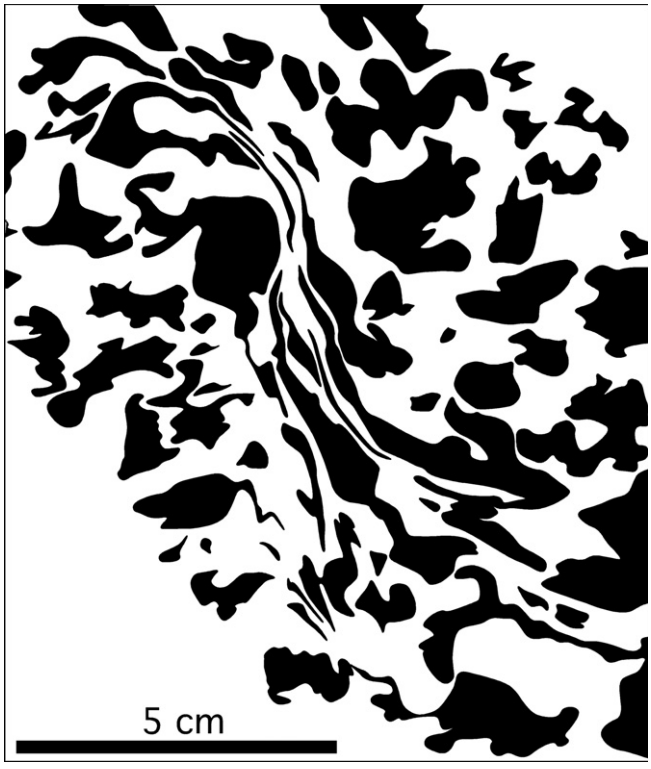

Fig. 10. Drawing of isolated shears found inside lozenges. These shears might be the result of deformation accommodation to maintain strain compatibility during bulk shearing. Black patches correspond to mafic minerals. North is upwards.

An explanation in accordance with the above arguments is that the conjugate shear system formed under a pure shear-dominated dextral transpression. Under such a tectonic regime, a majority of synthetic shear zones would form at low angle to the shear plane while minor antithetic shears formed at a high angle to the shear plane. Thus, we interpret that the present-day orientation of the main shear plane is close to NW–SE (Fig. 11b), i.e., roughly parallel to the boundaries of the Grassy Portage sill at the study site (Fig. 1) and that the bulk finite shortening direction lies between NNE and NE.

The current orientations of the shear zones and the deduced kinematic framework are apparently not compatible with the NW–SE directed dextral transpression determined from other studies (Poulsen, 2000; Czeck and Hudleston, 2003; Czeck et al., 2006), but in accordance with the strain analysis performed by Druguet et al. (2008) from deformed granitic veins in the area, that also gave a NNE shortening direction for the outcrops located NE of the Rice Bay dome (see Fig. 15 in Druguet et al., 2008). Possible explanations are that either the studied shear zones, located at the short limb of a large fold wrapping around the Rice Bay dome, experienced local stress field perturbation during a bulk NW–SE directed dextral transpression, or, alternatively, at least part of the folding event post-dated shear zone development, that is, involving a counterclockwise whole rock mass rotation of about 40–50°.

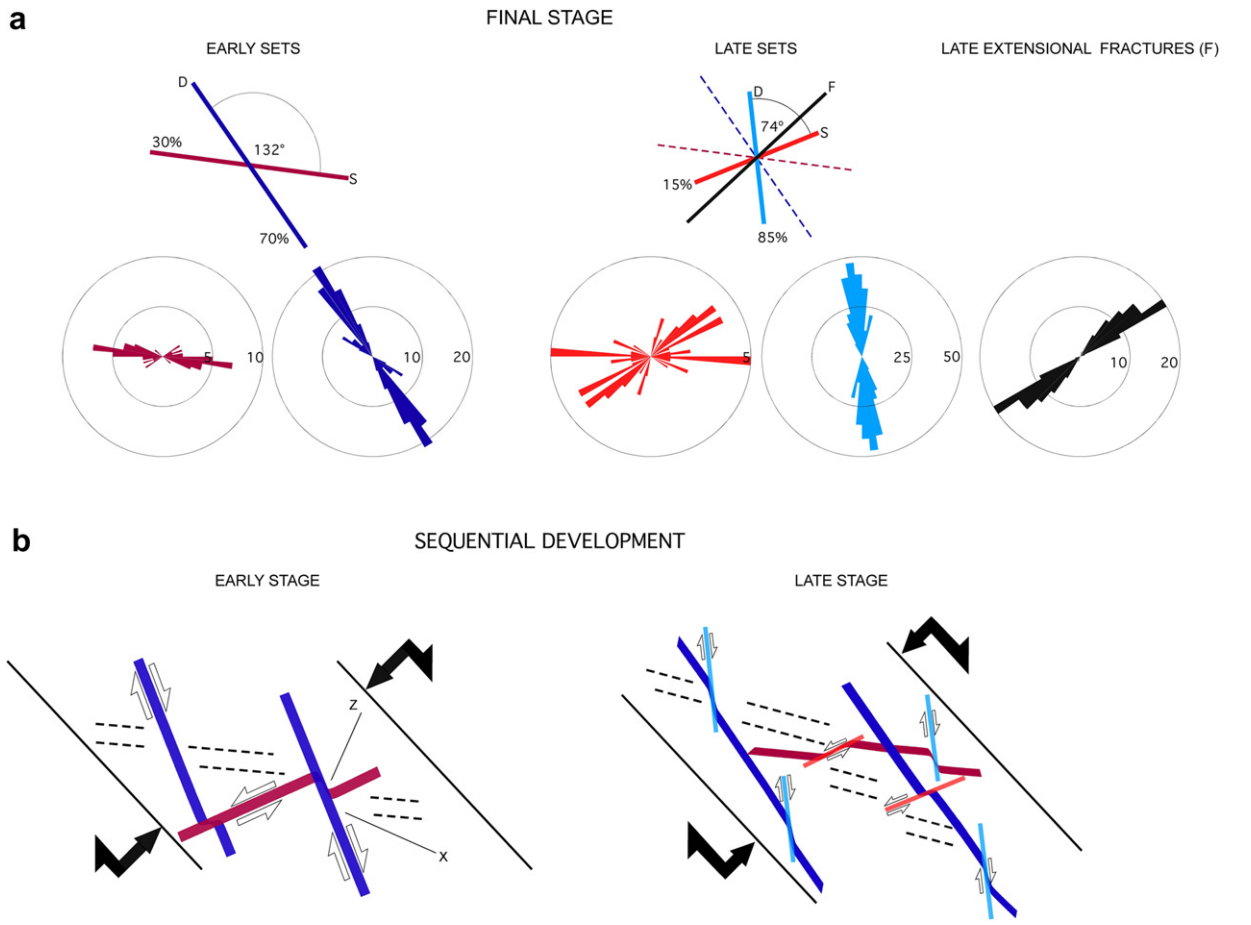

Fig. 11. (a) Mean orientation in plan view outcrop of the early and late dextral (*D*) and sinistral (*S*) sets of shears and corresponding Rose diagrams. The finite bulk shortening direction faces the obtuse angle between the sets. In both stages, dextral shears dominate over the sinistral ones, as indicated by the percentages. The orientation and corresponding Rose diagram of the late fractures (*F*) is also included. (b) Model for the sequential development of shears, drawn on the *XZ* plane with north upwards. In addition to shears, the orientation of the bulk *X* and *Z* directions, the assumed shear plane and the trend of the pre-existing foliation (dashed lines) have been drawn. It is assumed that the initial angle that faced the bulk shortening direction between sets was ~90°. As deformation progressed, the two sets rotated in opposite directions, and the angle between them increased. The later development of new dextral and sinistral sets led to complex coalescences and cross-cutting relationships. The fractures indicate that the late shortening direction was approximately parallel to the finite bulk shortening direction.

4.3. Alternative kinematic interpretations

Thus far, we have considered a kinematic interpretation that assumes that all features were formed during an almost constant stress regime. However, it is possible that this may not be the case if either i) multiple deformation events with different stress orientations formed the shear zones or ii) the rock rigidly rotated with respect to the bulk stresses during deformation, as in the case of a fold limb. If either case occurred, one would expect to see more complicated patterns of shear reactivations described for other regions (Bell, 1986; Ham and Bell, 2004).

In the case of the shear zone network considered here, it is unlikely that multiple deformation events were responsible for the shear zone patterns. All of the deformation in the region has been attributed to a N–S shortening event associated with dextral transpression (Poulsen et al., 1980; Poulsen, 1986, 2000; Davis et al., 1989; Czeck and Hudleston, 2003; Druguet et al., 2008) and there is no reason to suggest that there would have been younger events with different bulk stress orientations. In this limited outcrop, the local stress orientations are different than the bulk regional stress orientations, but the continuity of foliations between this outcrop and the region suggest that the local deflection of stresses is due to wrapping of foliation around the nearby Rice Bay Dome, which was presumably more competent, rather than a different bulk stress. It is possible that the rock was rotated with respect to the bulk regional stress during deformation because the rock may have been folded around the Rice Bay Dome during the shear zone network formation. If that were the case, the shear zone network pattern may have been formed during different relative stress orientations and shears would be reactivated during various stages of rotation, similar to the situation described by Bell (1986) and Ham and Bell (2004). However, because there are multiple cross-cutting relationships between sinistral and dextral faults, we prefer the simpler interpretation of the entire network forming within constant relative stress orientations.

5. Conclusions

This case study shows the development of a network of anastomosed shear zones arising from conjugate shears with a prevalent dextral set. The intersections and confluences of the shear zones indicate a complex deformation history, with dextral and sinistral shears being active together or intersecting, in an alternating fashion. In spite of this complexity, a twofold distinction between early and late shear sets has been adopted. The thicker shear zones of dextral and sinistral sense formed first, and mutually cross cut one another indicating their overall coeval development.

The latest shear zones are narrow, rather straight, and offset the earlier ones. The most important points of this analysis are:

(1) The observed pattern of the obtuse angle between the earliest shear zone sets facing the shortening direction is not an original feature but one that was achieved by progressive rotation of shears. The rotation was achieved by internal deformation of the lozenges with new shears forming inside and new shears that nucleated at the shear zone boundaries and propagated towards the lozenge interior.
(2) The kinematic analysis is consistent with the formation of the shear zone sets at nearly right angles. The earlier shear zones became reoriented by rotation during the subsequent bulk deformation of the rocks, involving displacement on later shear zones and deformation of the lozenges bounded by shear zones. The bulk deformation that produced the reorientation of the early shear zones was not homogeneous, as a horizontal shortening of about 45% is needed to produce the inferred rotation. The cores of many of the lozenges do not reflect a deformation of this intensity.
(3) The bulk deformation was noncoaxial, as dextral shear zones predominate over sinistral especially in later stages, although anisotropy of the rock may have contributed to the preferential development of dextral shears. This unequal development and evolution of both sets is coherent with a deformation regime evolving from a pure shear-dominated dextral transpression to a higher vorticity dextral transpression.
(4) The final phase of deformation involved brittle extensional fracturing of anorthositic pods under a uniform stress field. The extension direction inferred from these final features is at a small angle to the finite stretching direction, suggesting a quasi-steady orientation of the principal strain axes throughout the deformation history.

Acknowledgements

This work was funded by the Spanish Ministry of Education and Science (projects CGL2004-03657/BTE and CGL2007-66857-C02-01). The manuscript was mainly developed during a research stay of J.C. at the University of Wisconsin-Milwaukee, funded by the "Generalitat de Catalunya-AGAUR Agency" (2008 BE-1 0023). We are grateful to Lina Marcela Castaño for field support and photo-mosaic composition, and to Marcel Druguet who helped with brushing the outcrop. We thank Tim Bell and an anonymous reviewer for their comments and Editor Tom Blenkinsop for his assistance.

References

Alsop, G.I., Holdsworth, R.E., 2002. The geometry and kinematics of flow perturbation folds. Tectonophysics 350, 99–125.
Arbaret, L., Hussain, S., Dawood, H., Burg, J.-P., Zeilinger, G., Chaudhry, N., 2000. Pre-collisional anastomosing shear zones in the Kohistan arc, NW Pakistan. In: Khan, M.A., Treloar, P.J., Searle, M.P., Jan, M.Q. (Eds.), Tectonics of the Nanga Parbat Syntaxis and the Western Himalaya. Geological Society, London, Special Publications, vol. 170, pp. 295–311.
Bell, T.H., 1978. Progressive deformation and reorientation of fold axes in a ductile mylonite zone: the Woodroffe thrust. Tectonophysics 44, 285–298.
Bell, T.H., 1981. Foliation development: the contribution, geometry and significance of progressive, bulk, inhomogeneous shortening. Tectonophysics 75, 273–296.
Bell, T.H., 1986. Foliation development and refraction in metamorphic rocks: reactivation of earlier foliations and decrenulation due to shifting patterns of deformation partitioning. Journal of Metamorphic Geology 4, 421–444.
Bhattacharyya, P., Czeck, D.M., 2008. Using network analyses within GIS technologies to quantify geometries of shear zone networks. Geosphere 4, 640–656.
Bhattacharyya, P., Hudleston, P.J., 2001. Strain in ductile shear zones in the Caledonides of northern Sweden; a three-dimensional puzzle. Journal of Structural Geology 23, 1549–1565.
Borradaile, G.J., Dehls, J.F., 1993. Regional kinematics inferred from magnetic subfabrics in Archean rocks of northern Ontario, Canada. Journal of Structural Geology 15, 887–894.
Borradaile, G.J., Werner, T., Dehls, J.F., Spark, R.N., 1993. Archean regional transpression and paleomagnetism in northwestern Ontario, Canada. Tectonophysics 220, 117–125.
Burg, J.-P., Ricou, L.-E., Ivanov, Z., Godfriaux, I., Dimov, D., Klain, L., 1996. Syn-metamorphic nappe complex in the Rhodope Massif: structure and kinematics. Terra Nova 8, 6–15.
Card, K.D., Ciesielski, A., 1986. DNAG subdivisions of the superior province of the Canadian shield. Geoscience Canada 13, 5–13.
Carreras, J., Losantos, M., 1982. Geological setting of the Roses granodiorite (E-Pyrenees, Spain). Acta Geologica Hispanica 17, 219–225.
Carreras, J., 2001. Zooming on northern Cap de Creus shear zones. Journal of Structural Geology 23, 1457–1486.
Carreras, J., Druguet, E., Griera, A., 2000. Desarrollo de zonas de cizalla conjugadas por deformación coaxial de materiales analógicos anisótropos. Geotemas 1 (1), 47–52.
Carreras, J., Druguet, E., Griera, A., Soldevila, J., 2004. Strain and deformation history in a syntectonic pluton. The case of the Roses granodiorite (Cap de Creus, Eastern Pyrenees). In: Alsop, G.I., Holdsworth, R.E., McCaffrey, K.J.W., Hand, W. (Eds.), Flow Processes in Faults and Shear Zones. Geological Society, London, Special Publications, vol. 224, pp. 307–319.
Carreras, J., Druguet, E., Griera, A., 2005. Shear zone-related folds. Journal of Structural Geology 27, 1229–1251.
Choukroune, P., Gapais, D., 1983. Strain pattern in the Aar granite (Central Alps): orthogneiss developed by bulk inhomogeneous flattening. Journal of Structural Geology 5, 411–418.
Cobbold, P.R., Cosgrove, J.W., Summers, J.M., 1971. The development of internal structures in deformed anisotropic rocks. Tectonophysics 12, 23–53.
Corsini, M., Vauchez, A., Caby, R., 1996. Ductile duplexing at a bend of a continental-scale strike-slip shear zone: example from NE Brazil. Journal of Structural Geology 18, 385–394.
Cundall, P., 1991. Shear band initiation and evolution in frictional materials. In: Mechanics Computing in 1990's and Beyond (Proceedings of the Conference, Columbus, Ohio, May 1991). Structural and Material Mechanics, vol. 2. ASME, New York, pp. 1279–1289.
Czeck, D.M., Hudleston, P.J., 2003. Testing models for obliquely plunging lineations in transpression: a natural example and theoretical discussion. Journal of Structural Geology 25, 959–982.
Czeck, D.M., Hudleston, P.J., 2004. Physical experiment of vertical transpression with localized nonvertical extrusion. Journal of Structural Geology 26, 573–581.
Czeck, D.M., Maes, S.M., Sturm, C.L., Fein, E.M., 2006. Assessment of the relationship between emplacement of the Algoman plutons and regional deformation in the Rainy Lake region, Ontario. Canadian Journal of Earth Sciences 43, 1651–1653.
Davis, D.W., Poulsen, K.H., Kamo, S.L., 1989. New insights into Archean crustal development from geochronology in the Rainy Lake area, Superior Province, Canada. Journal of Geology 97, 379–398.
Druguet, E., Alsop, G.I., Carreras, J., 2009. Coeval brittle and ductile structures associated with extreme deformation partitioning in a multilayer sequence. Journal of Structural Geology 31, 498–511.
Druguet, E., Czeck, D.M., Carreras, J., Castaño, L.M., 2008. Emplacement and deformation features of syntectonic leucocratic veins from Rainy Lake zone (Western Superior Province, Canada). Precambrian Research 163, 384–400.
Duebendorfer, E.M., Christensen, C.H., 1998. Plastic-to-brittle deformation of microcline during deformation and cooling of a granitic pluton. In: Snoke, A.W., Tullis, J.A., Todd, V.R. (Eds.), Fault-related Rocks: a Photographic Atlas. Princeton University Press, pp. 176–179.
Fralick, P., Purdon, R.H., Davis, D.W., 2006. Neoarchean trans-subprovince sediment transport in southwestern Superior Province: sedimentological, geochemical, and geochronological evidence. Canadian Journal of Earth Sciences 43, 1055–1070.
Fusseis, F., Handy, M.R., Schrank, C., 2006. Networking of shear zones at the brittle-to-viscous transition (Cap de Creus, NE Spain). Journal of Structural Geology 28, 1228–1243.
Gapais, D., Bale, P., Choukroune, P., Cobbold, P.R., Mahjoub, Y., Marquer, D., 1987. Bulk kinematics from shear zone patterns: some field examples. Journal of Structural Geology 9, 635–646.
Ghosh, S.K., Sengupta, S., 1987. Progressive development of structures in a ductile shear zone. Journal of Structural Geology 9, 277–287.
Gómez-Rivas, E., Griera, A., Carreras, J., Druguet, E., 2006. Influencia de la orientación de la anisotropía en el desarrollo de shear bands: estudio experimental. Geogaceta 40, 47–50.
Ham, A.P., Bell, T.H., 2004. Recycling of foliations during folding. Journal of Structural Geology 26, 1989–2009.
Harris, L.B., 2003. Folding in high-grade rocks due to back-rotation between shear zones. Journal of Structural Geology 25, 223–240.
Hudleston, P., 1999. Strain compatibility and shear zones: is there a problem? Journal of Structural Geology 21, 923–932.
Hull, J., 1988. Thickness-displacement relationships for deformation zones. Journal of Structural Geology 10, 431–435.
Jessell, M.W., Bons, P.D., Griera, A., Evans, L.A., Wilson, C.J.L., 2009. A tale of two viscosities. Journal of Structural Geology 31, 719–736.
Kim, Y.-S., Peacock, D.C.P., Sanderson, D.J., 2004. Fault damage zones. Journal of Structural Geology 26, 503–517.
Lamouroux, C., Ingles, J., Debat, P., 1991. Conjugate ductile shear zones. Tectonophysics 185, 309–323.
Maerten, L., Gillespie, P., Pollard, D.D., 2002. Effect of local stress perturbation on secondary fault development. Journal of Structural Geology 24, 145–153.

Mancktelow, N.S., 2002. Finite-element modelling of shear zone development in viscoelastic materials and its implications for localisation of partial melts. Journal of Structural Geology 24, 1045–1053.
Marquer, D., Challandes, N., Baudin, T., 1996. Shear zone patterns and strain distribution at the scale of a Penninic nappe: the Suretta nappe (Eastern Swiss Alps). Journal of Structural Geology 18, 753–764.
Means, W.D., 1995. Shear zones and rock history. Tectonophysics 247, 157–160.
Mitra, G., 1979. Ductile deformation zones in Blue Ridge basement rocks and estimation of finite strain. Geological Society of America Bulletin 90, 935–951.
Mitra, G., 1998. Anastomosing deformation zones. In: Snoke, A.W., Tullis, J., Todd, V. R. (Eds.), Fault-related Rocks: a Photographic Atlas. Princeton University Press, pp. 142–143.
Montomoli, C., Carosi, R., Frassi, C., Ardito, N., Carreras, J., Druguet, E., 2008. Shear partitioning across two parallel shear zones in Roses granodiorite (Eastern Pyrenees, Spain). Rendiconti Della Società Geologica Italiana 3, 569–570.
Olsson, W.A., Lorenz, J.C., Cooper, S.P., 2004. A mechanical model for multiply-oriented conjugate deformation bands. Journal of Structural Geology 26, 325–338.
Passchier, C.W., Trouw, R.A.J., 2005. Microtectonics, second ed. Springer-Verlag, Berlin, 366 pp.
Passchier, C., Coelho, S., 2006. An outline of shear-sense analysis in high-grade rocks. Gondwana Research 10, 66–76.
Pennacchioni, G., Mancktelow, N.S., 2007. Nucleation and initial growth of a shear zone network within compositionally and structurally heterogeneous granitoids under amphibolite facies conditions. Journal of Structural Geology 29, 1757–1780.
Percival, J.A., Sanborn-Barrie, M., Skulski, T., Stott, G.M., Helmstaedt, H., White, D.J., 2006. Tectonic evolution of the western superior province from NATMAP and Lithoprobe studies. Canadian Journal of Earth Sciences 43, 1085–1117.
Pollard, D.D., Aydin, A.A., 1988. Progress in understanding jointing over the past century. Geological Society of America Bulletin 100, 1181–1204.
Poulsen, K.H., Borradaile, G.J., Kehlenbeck, M.M., 1980. An inverted Archean succession at Rainy Lake, Ontario. Canadian Journal of Earth Sciences 17, 1358–1369.
Poulsen, K.H., 1986. Rainy Lake wrench zone: an example of an Archean subprovince boundary in northwestern Ontario. In: de Wit, M.J., Ashwal, L.D. (Eds.), Tectonic Evolution of Greenstone Belts Technical Report 86-10. Lunar and Planetary Institute, Houston, TX, pp. 177–179.
Poulsen, K.H., 2000. Archean metallogeny of the Mine Centre – Fort Frances area. Ontario Geological Survey Report 266.
Ramsay, J.G., Allison, I., 1979. Structural analysis of shear zones in an Alpinised Hercynian granite, Maggia Nappen, Pennine zone, Central Alps. Schweizer Mineralogische und Petrographische Mitteilungen 59, 251–279.
Ramsay, J.G., Graham, R.H., 1970. Strain variations in shear belts. Canadian Journal of Earth Sciences 7, 786–813.
Ramsay, J.G., 1980. Shear zone geometry: a review. Journal of Structural Geology 2, 83–99.
Ramsay, J.G., Huber, M.I., 1987. The Techniques of Modern Structural Geology. Folds and Fractures, vol. 2. Academic Press, London.
Schrank, C.E., Boutelier, D.A., Cruden, A.R., 2008. The analogue shear zone: from rheology to associated geometry. Journal of Structural Geology 30, 177–193.
Schwarz, H.U., Kilfitt, F.W., 2008. Confluence and intersection of interacting conjugate faults: a new concept based on analogue experiments. Journal of Structural Geology 30, 1126–1137.
Stockwell, C.H., 1982. Proposals for time classification and correlation of Precambrian rocks and events in Canada and adjacent areas of the Canadian shield. Part 1: time classification of Precambrian rocks and events. Geological Survey of Canada Papers 80–90, 135.
Tabor, J.R., Hudleston, P.J., 1991. Deformation at an Archean subprovince boundary, northern Minnesota. Canadian Journal of Earth Sciences 28, 292–307.
Treagus, S.H., Lan, L., 2000. Pure shear deformation of square objects, and applications to geological strain analysis. Journal of Structural Geology 22, 105–122.
van der Pluijm, B.A., Marshak, S., 2003. Earth Structure. W.W. Norton, New York.
White, S.H., Burrows, S.E., Carreras, J., Shaw, N.D., Humphreys, F.J., 1980. On mylonites and ductile shear zones. Journal of Structural Geology 2, 175–187.
Wilcox, R.E., Harding, T.P., Seely, D.R., 1973. Basin wrench tectonics. The American Association of Petroleum Geologists Bulletin 57, 74–96.
Williams, P.F., Price, G.P., 1990. Origin of kinkbands and shear-band cleavage in shear zones: an experimental study. Journal of Structural Geology 12, 145–164.